

Temporal Behavior of Electron and Neutral Hydrogen Density Profiles during NBI in the GAMMA 10 Tandem Mirror

KUBOTA Yuusuke, YOSHIKAWA Masayuki, NAKASHIMA Yousuke,
KOBAYASHI Takayuki, SAITO Masashi, OHKI Toshikazu, HIGASHIZONO Yuta,
ITAKURA Akiyosi, TSUNODA Satonobu and CHO Teruji
Plasma Research Center, University of Tsukuba, Ibaraki 305-8577, Japan

(Received: 9 December 2003 / Accepted: 6 May 2004)

Abstract

In GAMMA 10, a neutral beam injector (NBI) is used for fueling to a plasma in the central cell. We measured time dependent radial profiles of electron and neutral hydrogen densities during the neutral beam injection. A different behavior was observed between both density profiles just after the beginning of the neutral beam injection and those 10ms after the beginning of the neutral beam injection. It is thought that the gases which originate in C-NBI play an important role in the change of plasma parameters during NBI in GAMMA 10.

Keywords:

GAMMA 10, particle fueling, NBI, H_{α} , neutral hydrogen density

1. Introduction

A particle fueling into a magnetically confined plasma is necessary to increase and sustain the plasma density. Measurements of electron and neutral hydrogen densities are important to study the fueling effect, because the fueling causes a lot of neutral gas influx to a target plasma. In GAMMA 10, a neutral beam injector (NBI) is used for fueling to a plasma in the central cell [1]. Then we measured the time dependent radial profiles of electron and neutral hydrogen densities during the neutral beam injection by using a microwave interferometer and H_{α} line emission detectors. In this paper, we show the detailed behavior of those density profiles during the neutral beam injection and discuss their analytical results.

2. Experimental apparatuses

GAMMA 10 is a 27 m long tandem mirror plasma confinement device with a thermal barrier. It consists of a 5.6 m long axisymmetric central cell, two anchor cells for suppressing magnetohydrodynamic (MHD) instabilities which are located in both ends of the central cell. Two plug/barrier cells connected to the anchor cells for forming the plug and thermal barrier potentials. Figure 1 shows the schematic view of the GAMMA 10 tandem mirror. In the GAMMA 10 plasma, the confinement is achieved by not only a magnetic mirror configuration but also high potentials at the both plug/barrier cells. The potentials are produced by means of the electron cyclotron resonance heating (ECRH) at the plug/barrier cells. The main plasma is produced and heated by the ion cyclotron

range of frequency (ICRF) power deposition. In plasmas produced in the central cell, typical electron density, electron temperature and ion temperature are about $2 \times 10^{12} \text{ cm}^{-3}$, 80 eV and 5 keV, respectively.

The objective of neutral beam injector at the central cell (C-NBI) is to supply the energetic particle to the main plasma and plasma heating. The beam line of C-NBI is perpendicular to the plasma column. The maximum power of the ion source of C-NBI is 0.75 MW (25 kV and 30 A, 0.1sec). While anchor NBI (A-NBI) system sustains high-beta plasma in the anchor cell for MHD stability by the ion heating and fueling ions. The maximum power of the ion source of A-NBI is 1.75 MW (25 kV and 70 A, 0.1 sec).

The line-integrated electron density of the plasma is measured with the microwave interferometer. The interferometer mounted on the mid-plane of the central cell can be scanned along the Y-axis of GAMMA 10. The radial profile of electron density is obtained by using the Abel inversion.

H_{α} emissions are measured with H_{α} line emission detectors which consist of interference filters, focusing lenses, apertures, optical fibers and photomultiplier tubes (PMTs). Near the mid-plane of the central cell, vertical and horizontal arrays of H_{α} detectors are installed to measure the spatial profiles of H_{α} line-integrated brightness [2]. Each array has 12 channel detectors. The output signals from the PMTs are amplified and led to a CAMAC system. This system is absolutely calibrated by a standard lamp. H_{α} emissions along axial direction (Z-axis) are also measured at several locations

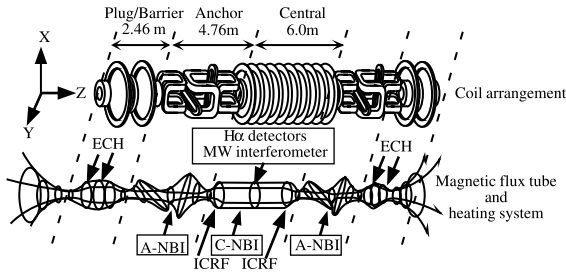


Fig. 1 The schematic view of the GAMMA 10 tandem mirror.

in GAMMA 10.

3. Calculation of neutral hydrogen density

Considering the asymmetric phenomena, we use an Algebraic Reconstruction Technique (ART) [3], which is the technique of reconstructing a local value from a line-integrated value. The explanation of ART is as follows. First we defined the mesh points as cross sections of line of sight of each channel. Initial values of those mesh points are given. Next, some mesh points are integrated along the line of sight in each channel. This integrated value is compared with measured data of its channel. This calculation is repeated until the integrated value will be in agreement with measured data in 5%. Then the 2-dimensional H_{α} line emission profile is obtained. The greatest advantage of ART compared with the Able inversion is that it is not necessary for ART to assume symmetry of plasma. The error in the ART is mainly based on the initial values, and the error is about 20%. The plasma presented in this paper is almost symmetry. Then we obtain the radial profiles of the H_{α} emissivity from the 2-dimensional profiles of the H_{α} emissivity obtained by ART. H_{α} emissivity is shown as below:

$$E(H_{\alpha}) = \frac{A_{32}\epsilon}{4\pi} n(3)_{exp}, \quad (1)$$

where A_{32} , ϵ , $n(3)_{exp}$ are the transition probability of H_{α} , the energy of H_{α} line emission and the population density of $n = 3$ of hydrogen atoms, respectively. The $n(3)_{exp}$ can be obtained experimentally from this eqs. (1). On the other hand, $n(3)_{CR}/n(1)_{CR}$ can be obtained as a function of electron density and electron temperature by using collisional-radiative model (CR-morel) [4-8], where $n(1)_{CR}$ is the population density of ground state of hydrogen atoms. Therefore the neutral hydrogen density can be obtained as

$$n_0 = \frac{n(3)_{exp}}{n(3)_{CR}} n(1)_{CR}. \quad (2)$$

Here n_0 is the neutral hydrogen density.

The effect of molecular hydrogen for H_{α} emission that originates a dissociative-excitation is about one tenth on the effect of hydrogen atom. The result of Monte Carlo simulation indicates that atom is still dominant for H_{α} emission even in the present plasma parameter range [9]. Therefore we

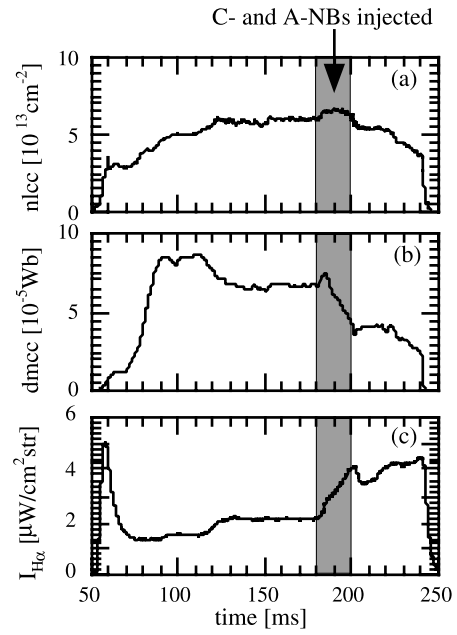


Fig. 2 Temporal behavior of line-integrated electron density (a), diamagnetism (b) and H_{α} line emission (c) at the central cell.

considered only the effect of hydrogen atom in this paper.

4. Experimental result

Temporal behaviors of the line-integrated electron density (a), the diamagnetism (b) and the H_{α} brightness of the central channel of vertical array (c) at the central cell are shown in Fig. 2. The plasma of this experiment is the ICRF-heated plasma with C-NBI and A-NBI as additional heating and particle fueling. The neutral beams in both the central and anchor cells are injected during 180 ms to 200 ms. In Fig. 2, bordering on 185 ms, the line-integrated electron density turns from the increase phase into the saturation phase, the diamagnetism turns from the increase phase into the decrease phase and the H_{α} brightness increases continuously during NBI. Therefore it is found that the change of phase occurs bordering around 185 ms. The time division from the beginning of NBI to 185 ms is defined to be the first phase and the second phase corresponds the division from 185 ms to the end of NBI.

At the first phase, the radial profiles of electron density and the neutral hydrogen density at 185 ms are shown in Fig. 3 (a). The density differences of these densities between before the NB injection (180 ms) and 185 ms are shown in Fig. 3 (b). At 185 ms, the electron density increases about 30 % in the peripheral region. The neutral hydrogen density decreases about 8 % in the peripheral region, and increases about 15 % in the central region. At the second phase, the radial profiles of electron and neutral hydrogen densities at 190 ms are shown in Fig. 4 (a). The density differences of these densities between 185 ms and 190 ms are shown in Fig. 4 (b). At 190 ms, the electron density increases about 10 % in the central region. The neutral hydrogen density increases

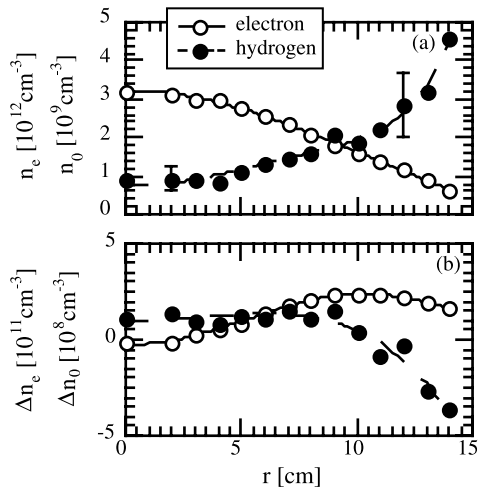


Fig. 3 (a) Radial profiles of electron and neutral hydrogen densities at 185 ms. (b) The density differences (185 ms ~ 185 ms) of these densities at the first phase.

about 25 % in the peripheral region.

The electron temperature is estimated about 50 – 100 eV in the central region and 20 – 30 eV in the peripheral region. The error on the neutral hydrogen density from the electron temperature uncertainty is several percent in the central region and that is 20% in the peripheral region. In Fig. 3 and Fig. 4, we show the error on the neutral hydrogen density which originates in the electron temperature uncertainty and ART.

5. Discussion

It is thought that there are three kinds of effects of NBI to the target plasma. These are the effects of the neutral beam itself, the recycling gas from vacuum vessel and the cold gas from NBI ion source. The effect of recycling gas indicates the effect by a change of recycling gas that is caused by the

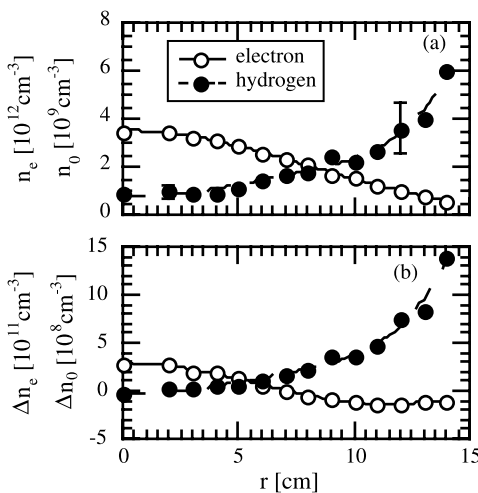


Fig. 4 (a) Radial profiles of electron and neutral hydrogen densities at 190 ms. (b) The density differences (185 ms ~ 190 ms) of these densities at the second phase.

beam–plasma interaction for example a charge exchange reaction. The effect of beam itself can't be observed directly, because the microwave interferometer and the H_α line emission detector arrays are 60–110 cm away from NBI beam line. While the time evolution of H_α brightness enables us to distinguish the effect of recycling gas from that of cold gas influx. As shown in Fig. 5 (we show the signal of the H_α detector installed on $Z = -123.5$ cm for example. The line of sight of this detector is on the beam line of C-NBI), the H_α brightness increases continuously after turning off the NBI pulse. This increase is caused by the cold gas. Its increasing rate is almost constant. The increase of H_α brightness, which is indicated by a slanted dashed-line in Fig. 5, defined as $\Delta H_\alpha(\text{cold gas})$. The increase of H_α brightness, which is over the line of cold gas, is defined as $\Delta H_\alpha(\text{recycling gas})$. The $\Delta H_\alpha(\text{recycling gas})$ s and the $\Delta H_\alpha(\text{cold gas})$ s on each axial position at $t = 190$ ms are obtained and shown in Fig. 6. Those two kinds of gases are localized near the beam line as shown in Fig. 6. This observation shows the significant difference between the quantities of two kinds of gases near the beam line and the quantities of those gases around the detectors. Therefore it is necessary to consider separately near the beam line and around the detectors.

At the first phase, the increase of electron density in the peripheral region is explained as follows: The recycling gas increases and the cold gas influx is caused by neutral beam injection. The neutral hydrogen increases at outside of the plasma by these gases. This hydrogen penetrates into the plasma and is ionized by electron impact. Therefore electron density increases in the peripheral region. These gases can't

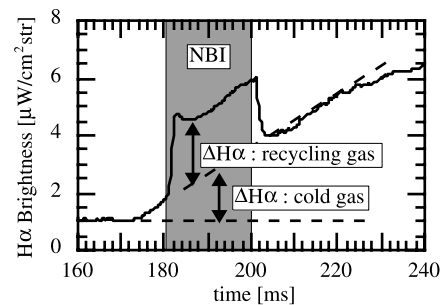


Fig. 5 The example of the effects of recycling gas and cold gas on the H_α brightness. ($Z = -123.5$ cm; line of sight of this H_α detector is on the beam line of C-NBI)

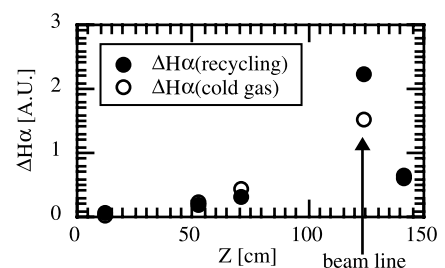


Fig. 6 The effect of recycling and cold gases at 190 ms on each position.

penetrate into the central region of the plasma. The decrease of the neutral hydrogen density in the peripheral region is also explained as follows: An electron density increases near the beam line. The electron flows along the magnetic field line quickly. However the recycling gas and the cold gas flow slowly compared with the electron flow. The mean free path of neutral hydrogen atom (12 cm at 180 ms) in the peripheral region is reduced to 9 cm at 185 ms in the peripheral region. Therefore around the detectors, neutral hydrogen is ionized by electron impact in the peripheral region, however neutral gas influx doesn't increase. Then the neutral hydrogen density decreases in the peripheral region.

At the second phase, the increase of electron density in the central region is explained as follows: An electron density increases by A-NBI near the mid-plane of the anchor cell. The electron flows along the magnetic flux from the anchor mid-plane to around the detectors at the central cell. Then the electron density at the central cell increases in the central region. However the electron density in the peripheral region doesn't increase. The reason is shown as below: The plasma produced in the anchor cell must flow through the non-axisymmetric anchor transition region. In peripheral region of the anchor transition region, the loss of the plasma is caused by the gradient- B drift [10]. The effect of the gradient- B drift in the peripheral region is large compared with the central region because the gradient- B in the peripheral region is larger. While, a clear asymmetry isn't observed in the central region. Also $n_e(\text{cm}^{-3}) / S(\text{particles}/\text{cm}^3\text{sec})$, which is defined as the indication of the particle confinement time in the local position, in the central region ($r = 0$ cm) is 4 times larger than that in the peripheral region ($r = 12$ cm). Here n_e and S are the electron density and the local ionization rate ($S = n_e n_0 \langle \sigma v \rangle_{\text{ioni}}, \langle \sigma v \rangle_{\text{ioni}}$: the electron impact ionization rate coefficient of the neutral hydrogen atom), respectively. Therefore in the peripheral region, electron density doesn't increase. On the other hand, the increase of the neutral hydrogen density in the peripheral region is also explained as follows: The recycling gas and the cold gas from ion source increases continuously near the beam line. These gases flow into the around of the detectors. Therefore the neutral hydrogen density increases in the peripheral region.

From above results, the changes of plasma parameters during NBI are explained by the recycling gas, the cold gas from ion source and the effect of A-NBI. Therefore from a viewpoint of the behavior of electron and neutral hydrogen densities, the phase change is caused by the two kinds of gases which originate in C-NBI and the effect of A-NBI. Especially, it is thought that those gases play an important role in the change of plasma parameters during NBI.

6. Summary

We measured the time dependent radial profiles of electron and neutral hydrogen densities during the neutral beam injection by using the microwave interferometer and the H_α line emission detectors. It is found that the temporal behaviors of the electron and neutral hydrogen density profiles are different between the first phase (from NBI-on to 185 ms) and the second phase (from 185 ms to NBI-off). In these behaviors, it is thought that two kinds of gases which originate in C-NBI play an important role in the change of plasma parameters during NBI.

Acknowledgments

The authors would like to thank members of GAMMA 10 group of University of Tsukuba.

References

- [1] Y. Nakashima *et al.*, J. Nucl. Mater. **313-316**, 553 (2003).
- [2] M. Yoshikawa *et al.*, Trans. Fusion Technol. **35**, 273 (1999).
- [3] Albert Macovski, *Medical Imaging Systems* (PRENTICE-HALL, INC).
- [4] T. Fujimoto, J. Phys. Soc. Jpn. **47**, 265 (1979).
- [5] T. Fujimoto, J. Phys. Soc. Jpn. **47**, 273 (1979).
- [6] T. Fujimoto, J. Phys. Soc. Jpn. **49**, 1561 (1980).
- [7] T. Fujimoto, J. Phys. Soc. Jpn. **49**, 1569 (1980).
- [8] T. Fujimoto, J. Phys. Soc. Jpn. **54**, 2905 (1985).
- [9] Y. Nakashima *et al.*, J. Nucl. Mater. **196-198**, 493 (1992).
- [10] Y. Nakashima *et al.*, J. Nucl. Mater. **290-293**, 683 (2001).